Campbell response in type II superconductors under strong pinning conditions

R. Willa[1], V.B. Geshkenbein[1], R. Prozorov[2], and G. Blatter[1]
[1] *Institute for Theoretical Physics, ETH Zurich, 8093 Zurich, Switzerland and*
[2] *The Ames Laboratory and Department of Physics and Astronomy, Iowa State University, Ames, Iowa 50011, USA*
(Dated: August 5, 2015)

Measuring the *ac* magnetic response of a type II superconductor provides valuable information on the pinning landscape (pinscape) of the material. We use strong pinning theory to derive a microscopic expression for the Campbell length $\lambda_{\rm C}$, the penetration depth of the *ac* signal. We show that $\lambda_{\rm C}$ is determined by the jump in the pinning force, in contrast to the critical current j_c which involves the jump in pinning energy. We demonstrate that the Campbell lengths generically differ for zero-field-cooled and field-cooled samples and predict that hysteretic behavior can appear in the latter situation. We compare our findings with new experimental data and show the potential of this technique in providing information on the material's pinscape.

PACS numbers: 74.25.N-, 74.25.Op, 74.25.Wx, 74.25.Ha

Technologically useful superconductors are of second type and acquire their desired transport and magnetic properties through vortex pinning, i.e., vortices [1] get immobilized by material defects. The characterization of the pinning landscape (or pinscape) is of great importance but presents quite a formidable task. Measurements of *dc* transport properties, either dynamically through the current–voltage characteristic [2] or statically through magnetization [3], are standard techniques used to gain information on the pinscape. Similarly, the *ac* magnetic response of superconducting samples [4] provides insight into the shape of pinning potentials. Unfortunately, the relation between the measured penetration depth of the *ac* signal, the so-called Campbell length $\lambda_{\rm C}$, and the parameters of the pinscape is only known on a phenomenological level. In this letter, we present a microscopic derivation of the Campbell length within the framework of strong pinning theory, thereby providing access to microscopic parameters of pinning defects and substantially enlarging the scope of applications of this measurement technique.

Probing superconductors via their *ac* magnetic response goes back to the 60-ies and culminated in Campbell's work [4] which provided the first consistent explanation of the penetration phenomenon (see Refs. [5] for further developments): for small *ac* magnetic-field amplitudes $h_{\rm ac}$ and frequencies ω, vortices oscillate reversibly within their pinning potentials (described as harmonic wells $\alpha\, x^2/2$), with the external signal h_{ac} penetrating the sample on a distance $\lambda_{\rm C} \propto B/\sqrt{\alpha}$ of order micrometers. Later work by Lowell [6] and Campbell [7] provided a more quantitative but still phenomenological understanding within a model pinscape. Here, we make use of the strong pinning scenario allowing us to perform a quantitative and microscopic analysis of the *ac* magnetic response. In particular, we find the dependence of the Campbell penetration depth $\lambda_{\rm C}$ on the vortex state, e.g., the critical (Bean [3]) state with a linear vortex density gradient supporting the critical current density j_c or a field-cooled state with a constant induction B, and predict the occurrence of new hysteretic effects. The comparison with recent experiments [8] confirms our predictions.

We consider a geometry with the superconductor occupying the half-space $X > 0$, the magnetic induction $B(X,t) = B_0 + \delta B(X,t)$ directed along Z, and the screening current j flowing along Y (capital and lower case letters distinguish between macroscopic and microscopic coordinates). The equation of motion for the macroscopic vortex displacement $U(X,t)$ reads

$$\eta \partial_t U = F_{\rm L}(j,U) + F_{\rm pin}(X,U), \tag{1}$$

with the Lorentz force $F_{\rm L}$ balanced by dissipative and pinning forces (η denotes the viscosity [9]). The displacement $U(X,t)$ relates to the induction via $\delta B(X,t) = -B_0\, \partial_{\rm x} U(X,t)$ and is driven at the surface $X = 0$ by the small external field $h_{ac} \ll B_0$, $\delta B(0,t) = h_{\rm ac} e^{-i\omega t}$. The Lorentz force $F_{\rm L} = (j_0 + \delta j)B/c$ involves an *ac* component $\delta j = -c\partial_{\rm x}\delta B/4\pi$ and writing the pinning force $F_{\rm pin} = F_0 + \delta F_{\rm pin}$, with F_0 the force density in the initial vortex state balancing the *dc* Lorentz force $j_0 B_0/c$, we obtain the dynamical equation

$$\eta\partial_t U - (B_0^2/4\pi)\partial_x^2 U - \delta F_{\rm pin}(U) = 0. \tag{2}$$

Following [4], one assumes small oscillations of the vortices near the potential minima. This motivates the phenomenological Ansatz $\delta F_{\rm pin}(U) = -\alpha U$ for the pinning force density. Solving (2) for the displacement field,

$$U(X,t) = \lambda_{\rm C}(h_{ac}/B_0) e^{-X/\lambda_{\rm C}} e^{-i\omega t} \tag{3}$$

$$\text{with} \quad \lambda_{\rm C}^2(\omega) = B_0^2/4\pi(\alpha - i\omega\eta), \tag{4}$$

results in the Campbell length $\lambda_{\rm C} = \lambda_{\rm C}(\omega = 0) = (B_0^2/4\pi\alpha)^{1/2}$ at low frequencies.

Here, our goal is to derive an expression for $\delta F_{\rm pin}$ starting from a microscopic perspective. This can be done within the framework of strong pinning theory which goes back to work of Labusch [10] and Larkin and Ovchinnikov

[11], with recent further studies on the critical currents in strong and weak pinning scenaria [12], numerical simulations of vortex motion [13], and the current–voltage characteristic [14]; note that the qualitative framework of weak collective pinning theory [11] is not sufficient to develop a quantitative understanding of $\lambda_{\rm C}$.

Consider a representative vortex within the flux-lattice driven along x on a trajectory described through the asymptotic coordinate $\mathbf{r}_\infty = (x, b)$ at large $|z|$; the distance b along y is the impact parameter with respect to a defect at the origin. Within the strong pinning context, defects act individually, generating a pinning potential $e_p(r, z)$. Considering a trajectory with maximal pinning, i.e., $b = 0$ and including the deformation energy of the vortex, its total energy as a function of x takes the form (we assume a point-like defect with $e_p(x, z) = e_p(x)\delta(z)$ [12])

$$e_{\rm pin}(x) = \frac{1}{2}\bar{C}u(x)^2 + e_p[x + u(x)], \tag{5}$$

with $u(x)$ the microscopic displacement field in the plane $z = 0$, see Fig. 1, and $\bar{C}$ the effective elasticity of the vortex embedded within the lattice,

$$\bar{C}^{-1} = \frac{1}{2}\int \frac{d^3k}{(2\pi)^3}\frac{1}{c_{66}(k_x^2 + k_y^2) + c_{44}(\mathbf{k})k_z^2}. \tag{6}$$

Here, c_{66} and $c_{44}(\mathbf{k})$ denote shear and dispersive tilt moduli and proper integration in (6) provides the result $\bar{C} \sim (a_0^2/\lambda)\sqrt{c_{66}c_{44}(0)}$ with $a_0^{-2} = B_0/\Phi_0$ the vortex density ($\Phi_0 = hc/2e$ is the flux unit and λ the London penetration depth). Minimization of (5) with respect to u (at fixed x) generates the self-consistency condition

$$\bar{C}u(x) = f_p[x + u(x)] \tag{7}$$

for the displacement field $u(x)$, where $f_p(x) = -e_p'(x)$ is the bare force profile of the pinning defect, the prime denoting derivative with respect to x. The maximal slope in f_p' (realized at x_m) defines the regime of strong pinning [10]: for $\kappa \equiv [f_p'(x_m)]/\bar{C} > 1$, the condition (7) generates two stable solutions for the displacement field $u(x)$, a pinned and an unpinned branch, see Fig. 1. The condition $\kappa = 1$ is the famous Labusch criterion [10] separating strong pins with $\kappa > 1$ from weak pins when $\kappa < 1$.

Assuming a homogeneous random distribution of defects with small density n_p, the macroscopic pinning force density $F_{\rm pin}$ derives from averaging the pinning forces $f_p[x+u_{\rm o}(x)]$ over all positions $|x| < a_0/2$ within a lattice period, with $u_{\rm o}$ denoting the branch that is occupied with vortices. This occupation depends on the state preparation, e.g., for a Bean state with vortices driven along x, the occupation of the pinned branch extends over the interval $[-x_-, x_+]$, see Fig. 1, such as to produce the maximal force $F_{\rm pin} = F_c$,

$$F_c = n_p\langle f_{\rm pin}\rangle = n_p\frac{t_\perp}{a_0}\int_{a_0}\frac{dx}{a_0}f_{\rm pin}(x)|_{\rm o}, \tag{8}$$

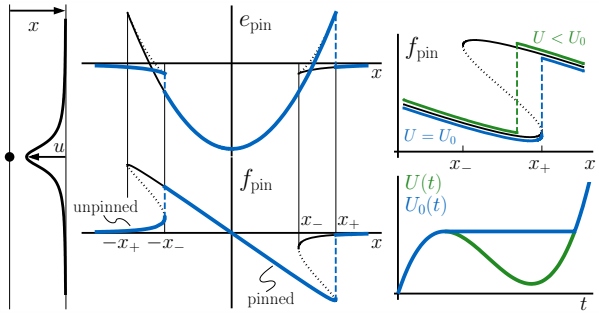

FIG. 1. Pinning energy $e_{\rm pin}$ and force $f_{\rm pin}$ in a strong pinning situation for a Lorentzian potential. The bistable solutions near the defect describe pinned and unpinned branches. Thick lines (blue) mark occupied branches in the Bean state, dotted lines are unstable solutions, dashed lines are the jumps making up for $\Delta e_{\rm pin}$ and $\Delta f_{\rm pin}$. Left: strong pinning situation for a representative vortex. The microscopic displacement $u(x) = f_{\rm pin}(x)/\bar{C}$ has the same shape as $f_{\rm pin}(x)$. Right: change in branch occupation when the vortex system moves by U.

where $f_{\rm pin}(x) \equiv f_p[x + u(x)]$ and $|_{\rm o}$ refers to the occupied branch $u_{\rm o}(x)$ (we assume maximal pinning for all trajectories with $2|b| < t_\perp \simeq \xi$, ξ the coherence length). Making use of the relation $f_{\rm pin}(x) = -de_{\rm pin}(x)/dx$, we arrive at a simple expression for the critical current density $j_c = (c/B)F_c$,

$$j_c = \frac{c}{B}n_p\frac{t_\perp}{a_0^2}\int_{a_0}dx\,[-de_{\rm pin}(x)/dx|_{\rm o}] = \frac{cn_pt_\perp}{\Phi_0}\Delta e_{\rm pin}, \tag{9}$$

where $\Delta e_{\rm pin}$ is the sum of jumps at $-x_-$ and x_+ in $e_{\rm pin}(x)$ where the occupation changes between unoccupied and occupied branches [10, 11], see Fig. 1.

Equipped with this microscopic understanding of pinned vortex matter in the Bean state, we return to the problem of *ac* magnetic response. Within strong pinning, we can follow the changes in the occupation of pinned and unpinned branches as vortices are driven by the *ac*-magnetic field and calculate the time dependent and inhomogeneous change in the pinning force $\delta F_{\rm pin}[U(x,t)]$. A macroscopic shift $U > 0$ pushes vortices in the direction of the Lorentz force; vortices at $-x_-$ and x_+ jump to pinned and unpinned branches, respectively, leaving the branch occupation unchanged, hence $\delta F_{\rm pin}(U > 0) = 0$. Otherwise, a negative displacement $U < 0$ shifts the boundaries between occupied and unoccupied states to the left, see Fig. 1. This results in a change of the macroscopic restoring force

$$\delta F_{\rm pin}(U<0) = n_p\frac{t_\perp}{a_0^2}\int_{a_0}dx[f_{\rm pin}(x)|_{{\rm o},U} - f_{\rm pin}(x)|_{{\rm o},0}], \tag{10}$$

where the index $|_{{\rm o},U}$ refers to the occupation where vortices have been shifted by U. Expanding the integrand

for small U, we arrive at the expression

$$\delta F_{\rm pin}(U<0) = n_p \frac{t_\perp}{a_0^2} \int_{a_0} dx\, df_{\rm pin}(x)/dx\big|_{\rm o}\, U, \qquad (11)$$

resulting in the strong pinning result for $\delta F_{\rm pin}$,

$$\delta F_{\rm pin}(U) \approx -n_p (t_\perp/a_0^2) \Delta f_{\rm pin}\, \Theta(-U)\, U, \qquad (12)$$

with $\Delta f_{\rm pin}$ the sum of jumps in the function $f_{\rm pin}$.

Inserting this result into Eq. (2) generates a complex vortex dynamics as flux enters the sample in a sequence of diffusive pulses until the field is raised to $B_0 + h_{ac}$, see [15] for a detailed description of this initialization process. After saturating the sample at this higher field level, the displacement $U(X,t)$ assumes the form

$$U(X,t) = U_0(X) - \lambda_{\rm C}(h_{ac}/B_0) e^{-X/\lambda_{\rm C}} [1 - e^{-i\omega t}], \quad (13)$$

with $U_0(X) = (h_{ac}/B_0)(L - X)$ generating the shift in field $B_0 \to B_0(1 - \partial_{\rm x} U_0) = B_0 + h_{ac}$ and L the penetration depth of the Bean profile [16]. The second term accounts for the penetration of the external field with respect to the *new* Bean state, $\delta B(X,t) = h_{ac} e^{-X/\lambda_{\rm C}}(1 - e^{-i\omega t})$. The Campbell penetration depth can be expressed by the microscopic parameters, the average curvature $d^2 e_{\rm pin}(x)/dx^2$, of the pinscape,

$$\frac{B_0^2}{4\pi\lambda_{\rm C}^2} = -\frac{n_p t_\perp}{a_0^2} \int_{a_0} dx\, d^2 e_{\rm pin}(x)/dx^2\big|_{\rm o} = \frac{n_p t_\perp}{a_0^2} \Delta f_{\rm pin}. \quad (14)$$

Making use of the estimates $\Delta f_{\rm pin} \sim f_p$, $t_\perp \sim \xi$, and $\kappa \sim f_p/\xi \bar{C}$, we find that $\lambda_{\rm C}^2 \sim \lambda^2/(\kappa n_p a_0 \xi^2) > \lambda^2$ with $\kappa\, n_p a_0 \xi^2 \ll 1$ the small parameter defining the three-dimensional strong pinning regime [12]. Comparing the results for j_c and $\lambda_{\rm C}^{-2}$, Eqs. (9) and (14), we observe that these two quantities address different properties of the pinscape, the jumps in pinning energy and force, respectively. As a consequence, the simple scaling $j_c \sim c\alpha\xi/B \sim (c/4\pi)\xi B/\lambda_{\rm C}^2$ previously conjectured on the basis of the phenomenological result (4) turns out incorrect and has to be replaced by $j_c \sim (c/4\pi)\kappa\xi B/\lambda_{\rm C}^2 \propto [\Delta f_{\rm pin}]^2$. Hence, care must be taken when translating measured data on $\lambda_{\rm C}$ into predictions for j_c [8].

Next, we turn to the field-cooled state with $j_0 = 0$ and $F_0 = 0$. Following (14), the determination of the jumps in the, now symmetric, occupation of $f_{\rm pin}$ is the central task in the calculation of $\lambda_{\rm C}$. Assuming defects in the form of metallic or insulating inclusions, one can show [15] that pinning turns on smoothly upon crossing the $H_{c2}(T)$ line. Hence, the vortex system changes from weak to strong pinning upon decreasing the temperature T below the Labusch temperature $T_{\rm L}$ defined through $\kappa(T_{\rm L}) = f_p'(x_m)/\bar{C}|_{T_{\rm L}} = 1$. At $T_{\rm L}$, the pinning force $f_{\rm pin}(x)$ develops an infinite slope at $x_{0{\rm L}}$, $[df_{\rm pin}/dx|_{x_{0{\rm L}}}]_{T_{\rm L}} = \infty$. Lowering the temperature below $T_{\rm L}$, the function $f_{\rm pin}(x)$ develops two branches, pinned and unpinned ones, which start and end at the boundaries $\pm x_+$ and $\pm x_-$ close to $\pm x_{0{\rm L}}$.

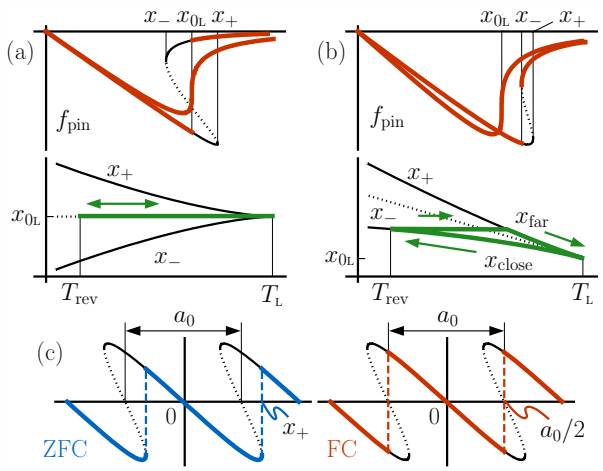

FIG. 2. Evolution of the pinning force $f_{\rm pin}$ crossing over from weak to strong pinning. The jump in the occupation between pinned and unpinned branches first appears at $x_{0{\rm L}}$ and remains there if the branch edges at $x_\pm$ move away in opposite directions with decreasing temperature, $x_- < x_{0{\rm L}} < x_+$, see (a). If $x_{0{\rm L}} < x_- < x_+$, see (b), the jump is pinned to x_- and hysteretic effects show up upon thermal cycling. (c) Pinscape $f_{\rm pin}(x)$ at high magnetic fields involving only pinned and unstable branches. The relevant jumps are located at x_+ for the zero-field-cooled sample (left) and at $a_0/2$ for the field-cooled situation (right).

In order to decide upon the branch occupation below $T_{\rm L}$, we have to determine the relative arrangement of the positions $x_{0{\rm L}}$ and $x_\pm$. We distinguish three cases, of which (a) is the simplest one, see Fig. 2(a), with $x_\pm$ moving away from $x_{0{\rm L}}$ in different directions. In this case, the branch occupation jumps between pinned and unpinned at $\pm x_{0{\rm L}}$ and a small *ac* field produces a small reoccupation around these points; the relevant jumps in $f_{\rm pin}$ thus appear at $\pm x_{0{\rm L}}$, with $\Delta f_{\rm pin} = 2\Delta f_{\rm pin}|_{x_{0{\rm L}}}$ entering the expression for the field-cooled Campbell length (14). Case (b) shown in Fig. 2(b) describes the situation where both branches grow beyond $x_{0{\rm L}}$ with decreasing temperature, $x_{0{\rm L}} < x_- < x_+$. Then, vortices between $x_{0{\rm L}}$ and x_- jump to the pinned branch and the relevant jump in the occupation is pinned to x_-. Accordingly, the jump in the pinning force entering $\lambda_{\rm C}$ is given by $2\Delta f_{\rm pin}|_{x_-}$. Finally, case (b') involves a shrinking of the branches with respect to $x_{0{\rm L}}$, i.e., $x_- < x_+ < x_{0{\rm L}}$, and the jump in occupation is pinned to x_+, $\Delta f_{\rm pin} = 2\Delta f_{\rm pin}|_{x_+}$. As a result, the Campbell length $\lambda_{\rm C}$ may differ for the zero-field-cooled (Bean type) and field-cooled vortex states in various respects, depending on the case at hand.

Quantitative analytic results can be obtained at temperatures below but close to $T_{\rm L}$ where $\kappa \gtrsim 1$. Expanding the bare pinning force $f_p(x)$ around x_m (where f_p'' vanishes), $f_p(x) \approx f_p(x_m) + f_p'|_{x_m}(x - x_m) - \gamma(x - x_m)^3/3$

with $2\gamma = -f_p'''|_{x_m} > 0$, we obtain the result

$$x_\pm = x_0 \pm \frac{2}{3}\sqrt{\frac{\bar{C}}{\gamma}}(\kappa-1)^{3/2}, \qquad (15)$$

with $x_0 = x_m - f_p(x_m)/\bar{C} > x_m$ the generalization of $x_{0\text{L}}$ to temperatures below T_L, $x_0(T_\text{L}) = x_{0\text{L}}$. The jumps at $\pm x_\pm$ then are equal and smaller than the jumps at $\pm x_{0\text{L}}$. For case (a), this results in different (by $\approx 7\%$) Campbell lengths $\lambda_\text{C}|_\text{FC} < \lambda_\text{C}|_\text{ZFC}$, while for the cases (b) and (b') the two lengths are equal. For large $\kappa \gg 1$, the three jumps are all different, resulting in different Campbell lengths with $\lambda_\text{C}|_{\text{FC}+} < \lambda_\text{C}|_\text{ZFC} < \lambda_\text{C}|_{\text{FC}-}$, where $\pm$ refer to the scenaria involving the large and small jumps at $x_\pm$.

Which of the above scenaria is realized in a specific case depends on the temperature dependence of elastic and pinning forces. Close to T_L, the behavior of $x_\pm$ is dominated by $x_0 \sim x_{0\text{L}} + a\tau_\text{L}$ with $\tau_\text{L} = 1 - T/T_\text{L}$ and the sign of the prefactor a deciding upon which case (b) or (b') is realized. On the other hand, for larger τ_L the second term in (15), $\propto (\kappa-1)^{3/2} \propto \tau_\text{L}^{3/2}$, becomes dominant and case (a) is realized.

Furthermore, hysteretic behavior of λ_C appears in cases (b) and (b') when first cooling and subsequently reheating the sample (from T_min). Indeed, when both branches increase or decrease below $x_{0\text{L}}$ upon cooling, the relevant jump appears at the branch edge x_close that is closer to $x_{0\text{L}}$. On reheating, the jump first remains pinned to $x_\text{close}(T_\text{min})$ until the other edge x_far further away from $x_{0\text{L}}$ is hit, whereupon the jump follows the position $x_\text{far}(T)$, see Fig. 2(b). Otherwise, in case (a) or when x_close goes through an extremum, no hysteresis appears upon thermal cycling as long as the jump in f_pin is realized [17] away from the branch edges at $\pm x_\pm$.

Next, we briefly discuss the situation at high fields when the pinned branch extends beyond the vortex separation a_0, $x_+ > a_0/2$. Close to H_{c_2}, the bare pinning force is well approximated by the lowest harmonic, $f_p(x) \approx f_0 \sin(2\pi x/a_0)$; the competition with elastic forces then produces the multi-valued function $f_\text{pin}(x)$ shown in Fig. 2(c). In this situation, the branch edges at $\pm x_-$ have vanished and only the pinned branches between $\pm x_+$ survive. For the Bean state, the jump in force ($\Delta f_\text{pin}|_{x_+}$) determining λ_C is located at x_+. For the field-cooled state, the (slightly larger) jump in force is located at $a_0/2$ instead, hence $\lambda_\text{C}|_\text{FC} \lesssim \lambda_\text{C}|_\text{ZFC}$; no hysteresis is expected in this regime. Upon decreasing the field, additional harmonics become relevant in the description of $f_p(x)$ and its maximal slope at x_m moves away from $a_0/2$, i.e., $x_m < a_0/2$. As $x_{0\text{L}}$ also decreases below $a_0/2$ an unpinned branch starts developing and we cross over to the low-field domain involving both the pinned and unpinned branches. Note that neither of these regimes is small but rather occupy similar size regions within the H-T phase diagram.

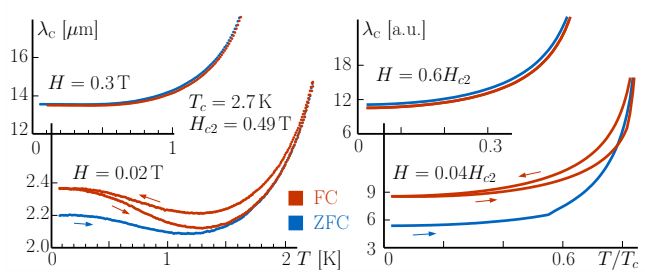

FIG. 3. Experimental (left) and theoretical (right) traces of the Campbell length $\lambda_\text{C}(T)$ for zero-field-cooled (blue) and (hysteretic) field-cooled (red) states at low (main panels) and high (inserted panels) magnetic fields.

In Fig. 3 we compare our main new findings, the dependence of λ_C on the vortex state and the appearance of hysteretic effects, with measurements on a single crystal superconductor $SrPd_2Ge_2$ (isostructural to the Fe- and Ni-pnictides) using a tunnel-diode oscillator technique, see Fig. 4(a) of Ref. [8] (shown are magnified traces at 0.02 T and 0.3 T). A small *ac* excitation field $h_{ac} \approx 20$ mOe is superimposed on the *dc* field ensuring linearity of the response, see Ref. [18] for experimental details. Theoretical results for the Campbell lengths are found by solving Eq. (7) and extracting the relevant jumps Δf_pin, assuming a pinning model based on insulating inclusions [15] (we use standard Ginzburg-Landau scaling). All features, the dependence of λ_C on the state preparation, the appearance of hysteresis upon thermal cycling, as well as the reversal from $\lambda_\text{C}|_\text{ZFC} < \lambda_\text{C}|_{\text{FC}-}$ at low fields to $\lambda_\text{C}|_\text{FC} < \lambda_\text{C}|_\text{ZFC}$ at high fields, are visible in the experiment and captured by the model; note that other pinning models based on metallic inclusions or δT_c-, $\delta\ell$-pinning [19] (ℓ the mean free path) produce different behavior.

In conclusion, making use of strong pinning theory, we have presented a microscopic and quantitative expression for the Campbell length λ_C that captures specific properties of the pinscape. Our theory predicts the dependence of λ_C on the vortex state (FC versus ZFC) and explains the appearance of hysteretic effects, with results that are in good agreement with experiments. With the new information at hand, the pinscape can be analyzed in much more detail via deliberate state preparation 'in between' the field- and zero-field-cooled extremes.

We acknowledge financial support of the Fonds National Suisse through the NCCR MaNEP. Research in Ames was supported by the U.S. DOE under contract #DE-AC02-07CH11358.

[1] A.A. Abrikosov, Sov. Phys. JETP **5**, 1174 (1957).
[2] A.R. Strnad, C.F. Hempstead, and Y.B. Kim, Phys. Rev. Lett. **13**, 794 (1964); Y.B. Kim, C.F. Hempstead, and

A.R. Strnad, Phys. Rev. **139**, A1163 (1965).
[3] C.P. Bean, Phys. Rev. Lett. **8**, 250 (1962).
[4] A.M. Campbell, J. Phys. C **2**, 1492 (1969), *ibid.* **4**, 3186 (1971).
[5] E.-H. Brandt, Z. Phys. B **80**, 167 (1990); M.W. Coffey and J. R. Clem, Phys. Rev. Lett. **67**, 386 (1991); A.E. Koshelev and V.M. Vinokur, Physica C **175**, 465 (1991); C.J. van der Beek, V.B. Geshkenbein, and V.M. Vinokur, Phys. Rev. B **48**, 3393 (1993).
[6] J. Lowell, J. Phys. F **2**, 547 (1972).
[7] A.M. Campbell, Philos. Mag. B **37**, 149 (1978).
[8] H. Kim, N.H. Sung, B.K. Cho, M.A. Tanatar, and R. Prozorov, Phys. Rev. B **87**, 094515 (2013).
[9] J. Bardeen and M.J. Stephen, Phys. Rev. **140**, 1197A (1965).
[10] R. Labusch, Cryst. Lattice Defects **1**, 1 (1969).
[11] A.I. Larkin and Yu.N. Ovchinnikov, J. Low Temp. Phys. **34**, 409 (1979), A.I. Larkin and Yu.N. Ovchinnikov, in *Nonequilibrium Superconductivity*, edited by D.N. Langenberg and A.I. Larkin (Elsevier, Amsterdam, 1986), p. 493.
[12] G. Blatter, V.B. Geshkenbein, and J.A.G. Koopmann, Phys. Rev. Lett. **92**, 067009 (2004).
[13] A.E. Koshelev and A.B. Kolton, Phys. Rev. B **84**, 104528 (2011).
[14] A.U. Thomann, V.B. Geshkenbein, and G. Blatter, Phys. Rev. Lett. **108**, 217001 (2012).
[15] R. Willa, V.B. Geshkenbein, and G. Blatter, *unpublished*.
[16] Note that within the phenomenological approach, the Bean critical state corresponds to a vanishing curvature $\alpha = 0$; the diverging $\lambda_C \to \infty$ can be attributed to vortices penetrating deep into the sample.
[17] At the minimum or maximum of $x_{\rm close}(T)$.
[18] R. Prozorov, R.W. Giannetta, N. Kameda, T. Tamegai, J.A. Schlueter, and P. Fournier, Phys. Rev. B **67**, 184501 (2003).
[19] G. Blatter, M.V. Feigel'man, V.B. Geshkenbein, A.I. Larkin, and V.M. Vinokur, Rev. Mod. Phys. **66**, 1125 (1994).